

## The Asteroid Veritas: An intruder in a family named after it?

Patrick Michel<sup>a,\*</sup>, Martin Jutzi<sup>b</sup>, Derek C. Richardson<sup>c</sup>, Willy Benz<sup>d</sup>

<sup>a</sup> University of Nice-Sophia Antipolis, CNRS, Observatoire de la Côte d'Azur, Cassiopée Laboratory, B.P. 4229, 06304 Nice Cedex 4, France

<sup>b</sup> Earth and Planetary Sciences, University of California, 1156 High Street, Santa Cruz, CA 95064, USA

<sup>c</sup> Department of Astronomy, University of Maryland, College Park, MD 20742-2421, USA

<sup>d</sup> Physicalisches Institut, University of Bern, Sidlerstrasse 5, CH-3012 Bern, Switzerland

### ARTICLE INFO

#### Article history:

Received 19 June 2010

Revised 19 October 2010

Accepted 19 October 2010

Available online 29 October 2010

#### Keywords:

Asteroids

Asteroids, Composition

Collisional physics

Impact processes

### ABSTRACT

The Veritas family is located in the outer main belt and is named after its apparent largest constituent, Asteroid (490) Veritas. The family age has been estimated by two independent studies to be quite young, around 8 Myr. Therefore, current properties of the family may retain signatures of the catastrophic disruption event that formed the family. In this paper, we report on our investigation of the formation of the Veritas family via numerical simulations of catastrophic disruption of a 140-km-diameter parent body, which was considered to be made of either porous or non-porous material, and a projectile impacting at 3 or 5 km/s with an impact angle of 0° or 45°. Not one of these simulations was able to produce satisfactorily the estimated size distribution of real family members. Based on previous studies devoted to either the dynamics or the spectral properties of the Veritas family, which already treated (490) Veritas as a special object that may be disconnected from the family, we simulated the formation of a family consisting of all members except that asteroid. For that case, the parent body was smaller (112 km in diameter), and we found a remarkable match between the simulation outcome, using a porous parent body, and the real family. Both the size distribution and the velocity dispersion of the real reduced family are very well reproduced. On the other hand, the disruption of a non-porous parent body does not reproduce the observed properties very well. This is consistent with the spectral C-type of family members, which suggests that the parent body was porous and shows the importance of modeling the effect of this porosity in the fragmentation process, even if the largest members are produced by gravitational reaccumulation during the subsequent gravitational phase. As a result of our investigations, we conclude that it is very likely that the Asteroid (490) Veritas and probably several other small members do not belong to the family as originally defined, and that the definition of this family should be revised. Further investigations will be performed to better constrain the definitions and properties of other asteroid families of different types, using the appropriate model of fragmentation. The identification of very young families in turn will continue to serve as a tool to check the validity of numerical models.

© 2010 Elsevier Inc. All rights reserved.

### 1. Introduction

In this paper, we investigate the formation of the Veritas asteroid family by numerical simulations of catastrophic disruption of a parent body considered to be made of either porous or non-porous material. The Veritas family is located in the outer main belt and is named after its apparent largest constituent, Asteroid (490) Veritas. Members of a family are believed to be fragments of a larger parent body that was disrupted by a catastrophic collision. Therefore, the study of asteroid families provides important information on the physics involved in collisional disruption and on the composition of main belt asteroids. Numerical simulations of catastrophic

disruptions that include both the fragmentation of the parent asteroid and the gravitational phase during which escaping fragments interact and can reaccumulate to grow larger bodies have been able to reproduce successfully some of the main asteroid families (Michel et al., 2001, 2002, 2003, 2004a,b; Durda et al., 2007). However, the model of fragmentation used in these simulations was only adapted to bodies in which microporosity was absent, and therefore, to asteroid families of bright taxonomic classes (e.g. S), assumed to be formed from a non-microporous parent body. Later, a model of fragmentation of microporous materials was introduced and validated at laboratory scale (Jutzi et al., 2008, 2009). This model was first applied at large scale to reproduce the asteroid family Baptistina (Jutzi et al., 2010). However, although this family was assumed to be of C taxonomic type by Bottke et al. (2007), who suggested that it may be at the origin of the K/T impactor, further observations indicated that it may be heterogeneous and badly identified, and therefore, the numerical

\* Corresponding author. Present address: Observatoire de la Côte d'Azur, UMR 6202 Cassiopée/CNRS, B.P. 4229, 06304 Nice Cedex 4, France. Fax: +33 492 003 058.

E-mail addresses: [michelp@oca.eu](mailto:michelp@oca.eu) (P. Michel), [mjutzi@ucsc.edu](mailto:mjutzi@ucsc.edu) (M. Jutzi), [dcr@astro.umd.edu](mailto:dcr@astro.umd.edu) (D.C. Richardson), [wbenz@space.unibe.ch](mailto:wbenz@space.unibe.ch) (W. Benz).

study by Jutzi et al. (2010), as stated in their paper, was faced with uncertainties regarding the data with which simulations should be compared.

The Veritas family is in principle a good candidate for comparing observations with numerical simulations, because its age has been estimated by two independent studies to be quite young, around 8 Myr (Nohakovic et al., 2010; Tsiganis et al., 2007; Nesvorný et al., 2003). Therefore, its current properties may still be close enough to those resulting from the catastrophic disruption of its parent body, and can thus be compared directly with the outcome of numerical simulations of this process. However, the Veritas family is not in a dynamically ‘quiet’ region of the main belt. In particular, the Asteroid (490) Veritas itself evolves on a chaotic orbit, as first pointed out by Milani and Farinella (1994), due principally to the action of the (5, −2, −2) Jupiter–Saturn–asteroid three-body resonance (Nesvorný and Morbidelli, 1998, 1999). Other family members have been identified to evolve chaotically (see, e.g., Milani and Farinella, 1994; Knezevic and Pavlovic, 2002), and this is the reason why Nesvorný et al. (2003) used only a sub-group of the family whose members appear to evolve on regular orbits to provide an age estimate. These authors then proposed that this age may either correspond to that of the whole family (as suggested by Tsiganis et al. (2007)), or to the age of the tight group of bodies on regular orbits around the second-largest member of the family, the Asteroid (1086) Nata. Then, Tsiganis et al. (2007) suggested that the Asteroid (490) Veritas and a large fraction of family members were substantially displaced from their original locations, due to chaotic diffusion, but that the young age was associated to the whole Veritas family. Therefore, because of the complex dynamics associated with this family, and different interpretations, both the family membership and the original member positions are not well determined, despite the young estimated age.

The Veritas family is classified as a dark type family whose members have spectral characteristics of low-albedo, primitive bodies, from C to D taxonomic types (Di Martino et al., 1997). Such types are usually believed to be composed of porous bodies (Britt and Consolmagno, 2000). Since we have now the ability to compute the catastrophic disruption of such kinds of bodies, we will use this asset in the following to investigate the outcome properties of such a disruption starting from the estimated size of the Veritas family parent body. This will allow us to check whether this outcome is consistent with the observed family properties, and to determine whether starting with either a porous or a non-porous parent body makes a difference. Then, as we will see, our investigation will actually lead to another possible scenario to explain this family, which may imply that the family should be re-defined.

In the following we first review our numerical models and discuss the material parameters that we used for our investigation (Section 2). Then we present the results from our simulations starting from the estimated size of the Veritas family parent body (Section 3). Section 4 explores an alternative scenario, which gives a surprisingly excellent match to observations, in which we remove the largest family member (Veritas itself) from the member list. These results are discussed in Section 5 and conclusions are presented in Section 6.

## 2. Numerical models and material parameters

In order to perform simulations of the Veritas family formation, we use a method and numerical codes based on those that have already allowed us to simulate successfully the formation of major bright-type asteroid families in different impact energy regimes (Michel et al., 2001, 2002, 2003, 2004a,b). More precisely, our method consists of dividing the process into two phases: a fragmentation phase computed by a hydrocode (Benz and Asphaug,

1994; Jutzi et al., 2008), and a gravitational phase computed by the gravitational *N*-body code *pkdgrav* (Richardson et al., 2000; Stadel, 2001) during which fragments can interact with each other due to their mutual gravity and collisions. The hydrocode was originally limited to addressing the fragmentation of brittle non-porous materials. While this is appropriate for modeling the formation of asteroid families of S taxonomic type, which are believed to result from the disruption of a non-microporous parent body, this model is not adapted for addressing the formation of asteroid families produced by microporous parent bodies, such as those of dark taxonomic type (e.g. C, D). In this case, a model of fragmentation of porous bodies (which accounts for the crushing of pores in addition to the damage caused by the activation of cracks) is required. Such a model has been developed and tested recently at laboratory scale (Jutzi et al., 2008, 2009). In the following we give a short overview of our method and codes, and then present our simulations.

### 2.1. Numerical models of fragmentation

#### 2.1.1. Classical model of brittle failure

To compute the fragmentation phase of the collision, we use a 3D smoothed-particle hydrodynamics (SPH) code (see e.g. Benz, 1990). The standard gas dynamics SPH approach was extended by Benz and Asphaug (1994, 1995) to include an elastic-perfectly plastic material description (see e.g., Libersky and Petschek, 1991) and a model of brittle failure based on that of Grady and Kipp (1980). The so-called Tillotson equation of state for basalt (Tillotson, 1962) is used to relate the pressure to density and internal energy. Material properties are also considered to be those of basalt, as they permit validation of the numerical model at laboratory scale (Benz and Asphaug, 1994) by comparison with impact experiments on basalt targets by Nakamura and Fujiwara (1991). We refer the reader to the paper by Benz and Asphaug (1994) for a detailed description of this code.

#### 2.1.2. Model including porosity

Recently, our SPH impact code has been extended to include a model adapted for porous materials (Jutzi et al., 2008, 2009). Before presenting its main principles, we first define what is meant here by porosity. The scale of porosity must be defined in comparison with the other relevant dimensions involved in the problem, such as the size of the projectile and/or crater. In particular, we define microscopic porosity as a type of porosity characterized by pores sufficiently small that their distribution can be assumed uniform and isotropic over these relevant scales. The sizes of the pores are in this case smaller than the thickness of the shock front. In this paper, a porous parent body is considered to contain such microporosity. Macroscopic porosity on the other hand is characterized by pores whose sizes are such that the medium can no longer be assumed to have homogeneous and isotropic characteristics over the scales of interest. In this case, pores have to be modeled explicitly and the hydrocode as described previously, which includes a model of non-porous brittle solids, can still be used. The presence of these large macroscopic voids will only affect the transfer efficiency and the geometry of the shock wave resulting from the impact, which can be computed using the original version of the hydrocode as done by Michel et al. (2003, 2004), who modeled the disruption of pre-shattered parent bodies of S-type families. On the other hand, a body containing microporosity may be crushable: cratering on a microporous asteroid might be an event involving compaction rather than ejection (Housen et al., 1999). Thus, in an impact into a microporous material, a part of the kinetic energy is dissipated by compaction, which can lead to less ejection and lower speeds of the ejected material. These effects cannot be reproduced if hydrocodes developed for the modeling of

non-porous solids are used, even if a low bulk density is given to the object. Therefore, a model is needed that takes pore compaction into account.

Our model is based on the so-called *P-alpha* model initially proposed by Herrmann (1969) and later modified by Carroll and Holt (1972). A detailed description of the model and its implementation in our SPH hydrocode can be found in Jutzi et al. (2008). The original idea at the origin of the *P-alpha* model is based on the separation of the volume change in a porous material into two parts: the pore collapse on one hand and the compression of the material composing the matrix on the other hand. This separation can be achieved by introducing the so-called distention parameter  $\alpha$  defined as  $\alpha = \rho_s/\rho$ , where  $\rho$  is the density of the porous material and  $\rho_s$  is the density of the corresponding solid (matrix) material. The distention  $\alpha$  can be converted to the porosity  $\Phi$  using the relation  $\Phi = 1 - 1/\alpha$ . The distention parameter  $\alpha$  is then used in the computation of the pressure and the deviatoric stress tensor. Damage increases as a result of both crack activation and change in the distension. As material parameters, we use those involved in our successful validation of the model by comparison with laboratory impact experiments on porous pumice (Jutzi et al., 2009).

## 2.2. Numerical model of the gravitational phase

Once the collision is over and fracture ceases, the hydrodynamical simulations are stopped and intact fragments (if any) are identified. These fragments as well as single particles and their corresponding velocity distribution are fed into an *N*-body code that computes the dynamical part of the evolution of the system to late time. Note that since the total mass is fixed, the extent of the reaccumulation is entirely determined by the velocity field imposed by the collisional physics upon the individual fragments. Since we are dealing with a fairly large number of fragments (typically a few hundreds of thousands) that we want to follow over long periods of time, we use the parallel *N*-body hierarchical tree code *pkdgrav* (Richardson et al., 2000; Stadel, 2001) to compute the dynamics. The tree component of the code provides a convenient means of consolidating forces exerted by distant particles, reducing the computational cost. The parallel component divides the work evenly among available processors, adjusting the load each timestep according to the amount of work done in the previous force calculation. The code uses a straightforward second-order leapfrog scheme for the integration and computes gravity moments from tree cells to hexadecapole order. Particles are considered to be finite-sized hard spheres and collisions are identified at each step using a fast neighbor-search algorithm. The code detects and treats collisions and mergers between particles on the basis of different options that were investigated by Michel et al. (2002) for monolithic parent bodies. Here we use a treatment in which a criterion based on relative speed and angular momentum is applied: fragments are allowed to merge only if their relative speed is smaller than their mutual escape speed and the resulting spin of the merged fragment is smaller than the threshold value for rotational mass loss. When two particles merge, they are replaced by a single spherical particle with the same momentum. Non-merging collisions are modeled as bounces between hard spheres whose post-collision velocities are determined by the amount of dissipation occurring during the collisions. The latter is determined in our simulations by the coefficients of restitution in the tangential and normal directions of the velocity vectors relative to the point of contact (see Richardson (1994) for details; also Richardson et al., 2009). The values of these coefficients are poorly constrained. In the following, we choose to set the normal coefficient of restitution to 0.3 in the porous case, and to 0.5 in the non-porous one, and the tangential coefficient to 1, meaning there is no coupling between spin and translational motion (see also Michel et al., 2002).

Note that we made a simulation using the value of 0.5 for the normal coefficient of restitution in the porous case, and found similar results to the ones found with the lower value. Michel et al. (2002) made simulations using a non-porous parent body and noted also that the outcomes were not sensitive to the adopted value of the normal coefficient set between 0.5 and 0.8.

All the *N*-body simulations presented in this paper were performed using a conservative integration step-size of 5 s and were run to late times from a few (simulated) days to a few tens of (simulated) days as indicated on the following plots, and at least until there was no further change in the outcome.

## 2.3. Material parameters and initial conditions

We considered two kinds of material composing the parent body of the Veritas family:

- Basalt (labeled non-porous).
- Pumice (labeled porous).

These two materials might not be the best representation of Solar System bodies. However, in contrast to other materials, in both cases these material parameters have passed successful comparison tests with laboratory impact experiments (Benz and Asphaug, 1995; Jutzi et al., 2009).

In addition to the two compositions, we considered two kinds of internal structures of the parent body. The first kind is a monolithic structure, which only contains incipient cracks whose distribution is provided by the Weibull parameters of the considered material, either basalt or pumice. The second kind is a pre-fragmented structure, which in addition to incipient cracks, is composed of large undamaged zones, separated by fully damaged particles (see Fig. 3 in Michel (2003), for an example). This serves as representing a body that has not suffered any disruption/reaccumulation process yet, but did suffer small impacts that pre-fragmented it. Indeed, the collisional lifetime of a body whose diameter is in the size range of the Veritas parent body (>100 km) makes it likely that the body was either monolithic or at most pre-fragmented when it was disrupted, and was not already a reaccumulated body from a previous disruption that transformed it into a rubble pile. Therefore, considering these two internal structures allows investigation of the collisional outcome from the most likely structures for the Veritas parent body.

## 3. Numerical simulations of the formation of the original Veritas family

In this section, we present the results of our numerical simulations of the disruption of the parent body of the Veritas family, whose diameter is 140 km (see Table 1 in Nesvorný et al., 2003). The initial conditions of the simulations are summarized in Table 1. All simulations were performed using about 200,000 particles to model the parent body. This results in a minimum size of particles between 1.07 and 1.35 km. The number of particles in the projectile was chosen to match the same mass per particle in the projectile as in the target.

We used the same bulk density for both the non-porous and porous parent bodies, so that they have the same mass, allowing a systematic comparison for a given specific impact energy. Because the Veritas family is classified as C-type, the chosen value of 1.3 g/cm<sup>3</sup> corresponds to the bulk density expected for C-type asteroids, as measured for the Asteroid Mathilde (Yeomans et al., 1997). We then considered two values of the projectile's speed consistent with the average impact speed in the main belt (Bottke et al., 1994).

**Table 1**

Impact conditions and largest remnant mass for all simulations using the original size of 140 km in diameter for the parent body. Both a non-porous or a porous composition were considered, and in both cases either a monolithic (M) or a pre-fractured (PF) internal structure was considered. The projectile's radius  $R_p$ , the impact speed  $V$ , the impact angle  $\theta$ , the specific impact energy  $Q$  and the mass ratio of the largest remnant to the parent body  $M_{lr}/M_{pb}$  obtained by our simulations are indicated.

Composition	Structure	$R_p$ (km)	$V$ (km/s)	$\theta$ (°)	$Q$ (erg/g)	$M_{lr}/M_{pb}$
Non-porous	M	12.3	5	0	$6.77 \times 10^8$	0.53
Non-porous	M	15.7	5	45	$1.41 \times 10^9$	0.47
Porous	M	12.3	5	0	$6.77 \times 10^8$	0.58
Porous	M	15.7	5	45	$1.41 \times 10^9$	0.56
Non-porous	PF	8.9	5	0	$2.58 \times 10^8$	0.66
Non-porous	PF	12.0	5	45	$6.25 \times 10^8$	0.47
Porous	PF	12.3	5	0	$6.77 \times 10^8$	0.57
Porous	PF	15.7	5	45	$1.41 \times 10^9$	0.58
Porous	M	20	3	45	$1.05 \times 10^9$	0.58

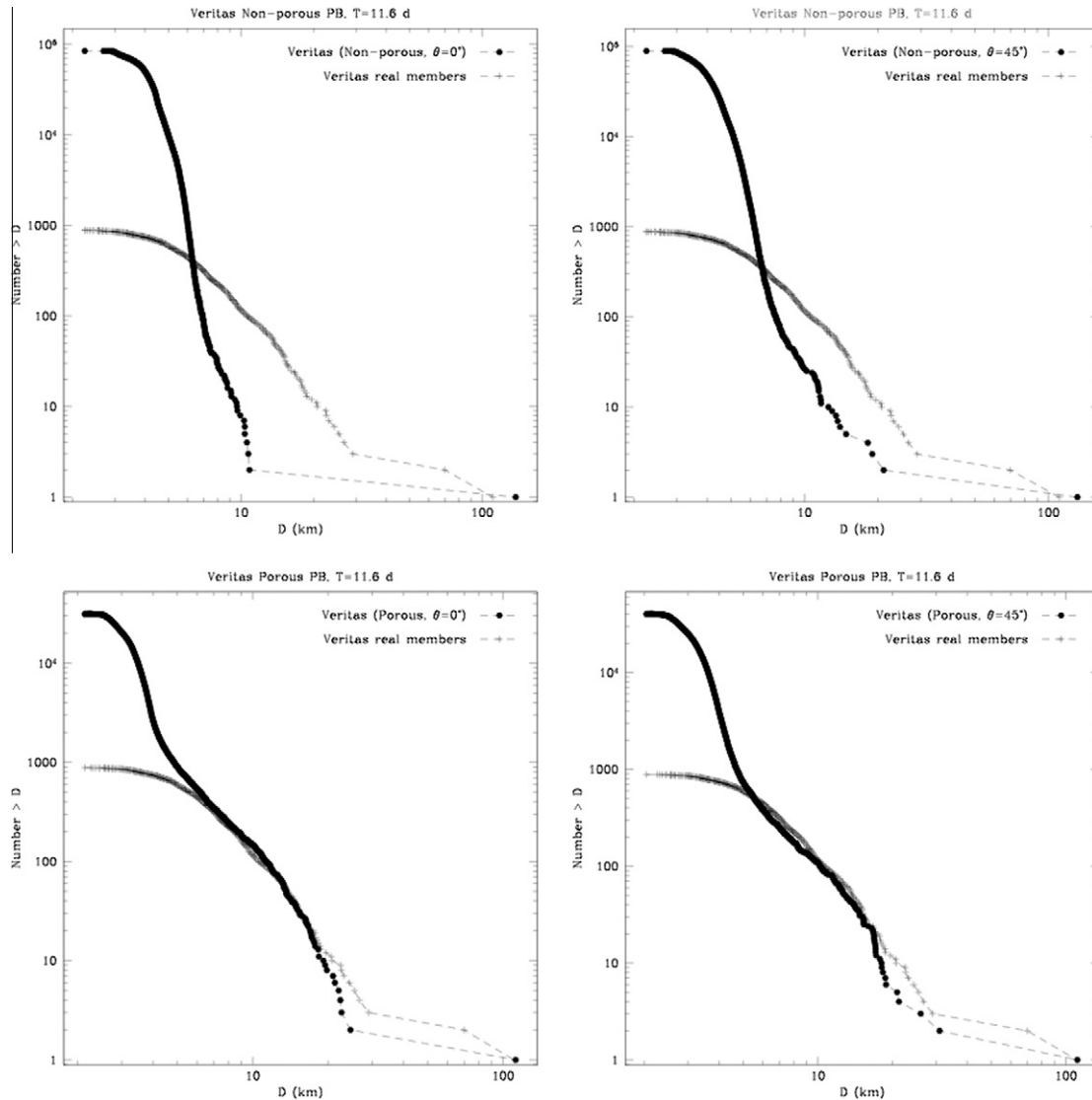
3.1. Size distribution of family members

Fig. 1 shows the size distributions of fragments resulting from the disruption of monolithic parent bodies. One can see that the outcome of the simulations starting with a non-porous parent

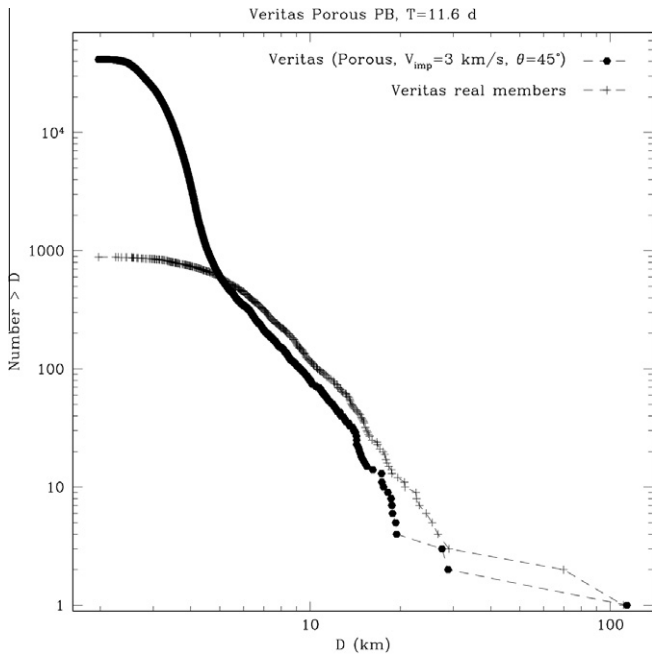
body lacks fragments at intermediate sizes and that the size distribution is therefore much more discontinuous than that of the real family. Simulations starting with a porous parent body result in a size distribution with a shape qualitatively similar to that of the real family. At first glance this appears satisfying, as using a porous parent body (and the corresponding model of fragmentation) is consistent with the taxonomic type of the family. However, while the simulations reproduce successfully the largest member, (490) Veritas, they do not reproduce the second-largest one, (1086) Nata, and there is too large a gap between the largest and second-largest fragments.

Fig. 2 shows a simulation starting with a porous parent body using an impact speed of 3 km/s and an impact angle of 45°. The outcome is qualitatively similar to the one from the 5 km/s impact (Fig. 1). Therefore, in the following, to reduce the parameter space, we will fix the impact speed at 5 km/s, which is the most likely value for main belt asteroids (Bottke et al., 1994).

Fig. 3 shows the size distributions of fragments resulting from the disruption of pre-fractured parent bodies. Although the gap between the largest and second-largest remnants is not as large as observed in the monolithic parent body cases, it is still too large



**Fig. 1.** Cumulative size distribution of fragments from the simulation of the disruption of a monolithic Veritas parent body (PB), either non-porous or porous, as indicated on the plots. Impact angles are 0° or 45° and the impact speed is 5 km/s. The size distribution of the real Veritas family is also shown for comparison. The simulated time is about 11.6 days after the impact.



**Fig. 2.** Cumulative size distribution of fragments from the simulation of the disruption of a monolithic porous Veritas parent body (PB). Impact angle is  $45^\circ$  and impact speed is 3 km/s. The size distribution of the real Veritas family is also shown for comparison. The simulated time is about 11.6 days after the impact.

to provide a good match to the real size distribution, in particular concerning the second-largest member of the family.

### 3.2. Orbital distribution of family members

We also characterized the outcome properties in terms of distribution in the orbital element space, as only the proper orbital elements (semi-major axis  $a$ , eccentricity  $e$ , and inclination  $I$ ) of the family members can be deduced from observations, whereas the simulations only provide the ejection velocities. However, Gauss' equations can be used to relate ejection velocities to orbital elements, provided the position of the barycenter of the family in a heliocentric reference frame is known. To solve these equations, two additional unknown angles must be specified, namely the true anomaly  $f$  and the argument of perihelion  $\omega$  of the parent body's orbit at the time of the impact. The current observed shape of the cluster in orbital element space suggests  $f = 30^\circ$  and  $\omega = 150^\circ$  as a good choice (Tsiganis et al., 2007).

Note also that the ejection velocities of our fragments are defined in the target's barycenter reference frame, with the  $z$ -axis in the direction of the projectile's impact velocity. In reality, this orientation of the projectile is improbable. To be more realistic, following our previous work (see, e.g., Michel et al., 2002), we considered main belt values as the orbital elements of the projectiles and used Öpik's theory (Öpik, 1951) to derive from these the direction of the impactor's velocity vector. Indeed, the impact velocity of the projectile fixes the so-called Tisserand parameter (see footnote 1 in Michel et al. (2002)), which in turn fixes the projectile's eccentricity, given the values of the semi-major axis and inclination of the projectile, and the value of the semi-major axis of the parent body. The direction of the impactor's velocity vector can then be determined using Öpik's geometry, which allows us to transform the components of the ejection velocities from the original reference frame to their components in the radial/along-track/out-of plane reference frame. A free parameter (the angle of the rotation matrix,  $\beta$  hereafter) must be arbitrarily fixed, which can influence the shape of the orbital dispersion. In the following  $\beta$  is set to  $90^\circ$ ,

and unless stated (see Section 4.2), other values do not change our conclusions.

Figs. 4 and 5 show the  $a$  vs.  $e$  and  $a$  vs.  $I$  distributions from our simulation using either a non-porous or a porous monolithic parent body. The impact speed and angle are 5 km/s and  $45^\circ$ , respectively. A curve of equivelocity is superimposed with a speed cutoff  $V_c = 40$  m/s.<sup>1</sup> This curve was used by Tsiganis et al. (2007) and Nohakovic et al. (2010) to represent the velocity dispersion of the real family. Small unobservable members may have been ejected at higher speeds, and to perform a consistent comparison, we only consider fragments produced in our simulations whose diameters are greater than 8 km. Note that the disruption of pre-fragmented parent bodies (both non-porous and porous) leads to the same dispersion as that of monolithic ones. However, the same plots for non-porous pre-fragmented parent body would contain more points (i.e. more fragments larger than 8 km) in the ellipses than we see in the plots of Fig. 4, as the size distribution of fragments from the disruption of non-porous pre-fragmented parent bodies contains a larger number of objects with size above 8 km (see, for comparison, Figs. 1 and 3, top-right plots).

The orbital dispersion produced by our simulation starting with a non-porous parent body leads to a better match with the dispersion of the real family than the one produced using a porous parent body. In the latter case, we find that the shape of the dispersion (irrespective of the chosen value of  $\beta$ ) in the  $a$ - $I$  plane is different from the real one, and the magnitude of the dispersion is also much larger, even when the impact speed is 3 km/s. Using an impact angle closer to  $0^\circ$  may provide a better match to the shape (see Section 4.2), but would not solve the discrepancy in the magnitude of the dispersion.

Although the match from the disruption of a non-porous Veritas parent body looks satisfying, the size distribution of fragments differs too much from the real one. Therefore, none of our simulations were found to reproduce both the size distribution and the velocity dispersion of the Veritas family. Obviously, the parameter space is large, and we cannot guarantee that some impact conditions or other models of the internal structure of the parent body would not lead to a good match; however, in the following we investigate another scenario that appears so successful that we believe that it is more likely to be the correct one.

## 4. Formation of the Veritas family without Veritas itself

Simulations presented in the previous section found a gap in the size distribution between the largest remnant and the second-largest one, which is not observed in the real family, where the second-largest member is the Asteroid (1080) Nata, whose diameter places it in this gap. Indeed, the orbit of (1086) Nata is regular and shows nodal convergence with a large fraction of family members at  $-8.3$  Myr (Nesvorný et al., 2003). The odds of showing convergence by chance are relatively small, therefore Nata cannot be considered to be an interloper. However, (490) Veritas and (1086) Nata are located on opposite sides of the family (3.174 AU and 3.165 AU, respectively), which could indicate either relatively large and not commonly seen separation speed between the two largest fragments or that one of these objects is an interloper. As mentioned above, Nata is not a good candidate to be an interloper. On the other hand, the orbit of (490) Veritas is chaotic and affected by

<sup>1</sup> Applying the Hierarchical Clustering Method (HCM, Zappalà et al., 1995) to identify the members of a family, the number of identified members depends on the value of the assumed speed cut-off that determines the maximum possible deviation of an asteroid's proper elements with respect to the 'central object' (usually the largest family member). This method, however, can artificially link asteroids with similar semi-major axis (such as those located in a resonance) but with a wide range of inclinations that can hardly be covered by a single disruption.

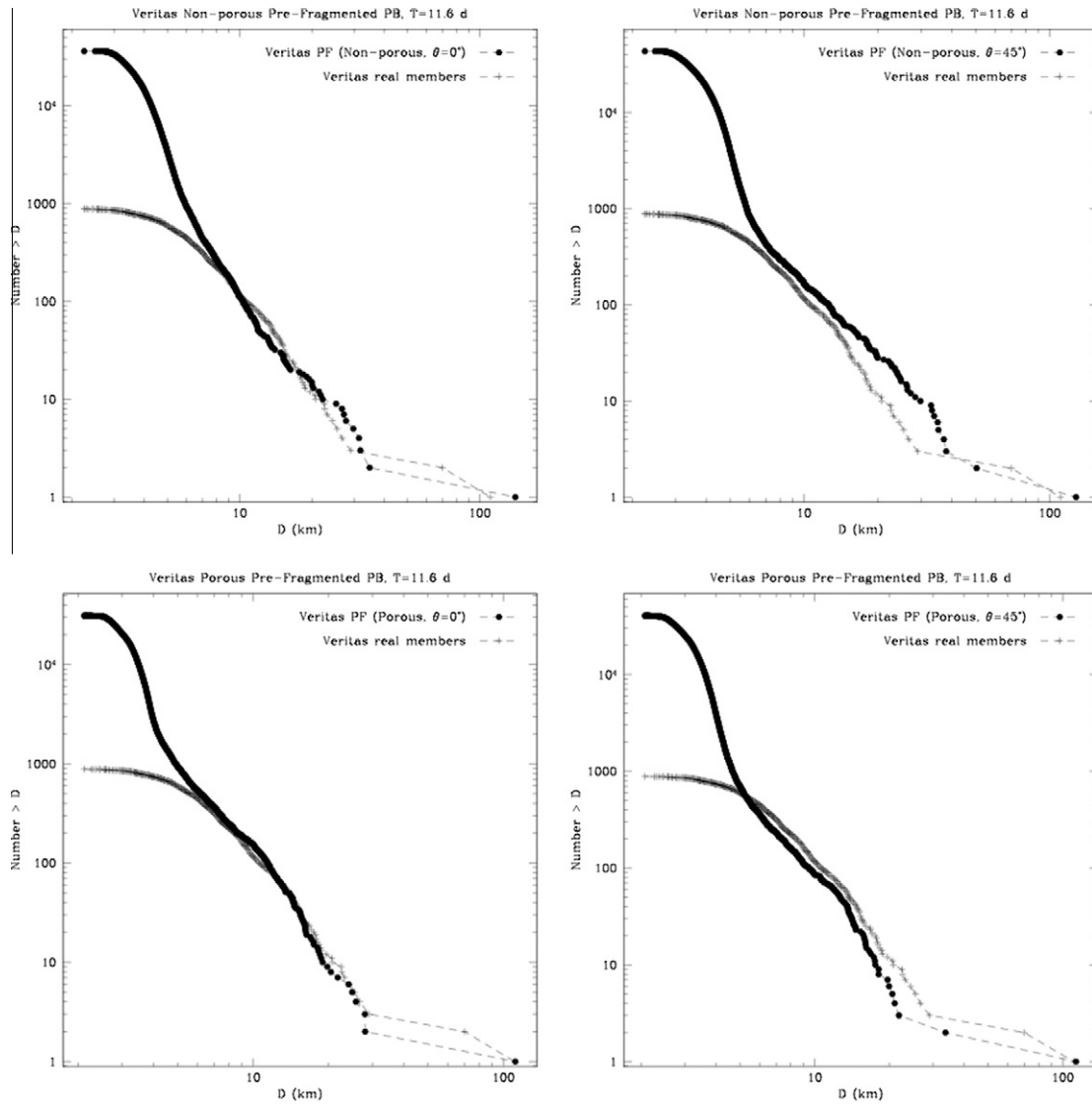


Fig. 3. Same as Fig. 1, starting with a pre-fragmented (PF) parent body (PB).

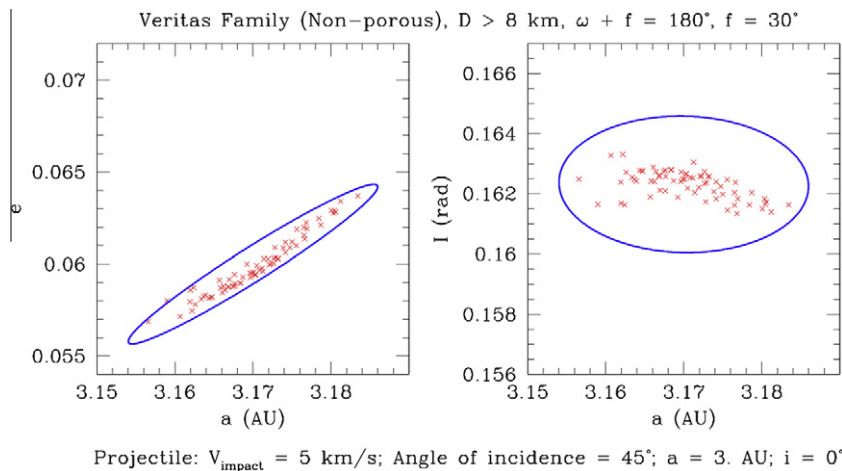


Fig. 4. Distribution of fragments larger than 8 km from our simulation of disruption of a non-porous monolithic parent body in the  $a-e$  plane (left) and  $a-I$  plane (right) as a result of the impact of a projectile at 5 km/s at 45° impact angle with orbital semi-major axis  $a$  of 3 AU and inclination  $I$  of 0°. The superimposed ellipse is an equivelocity curve for speed cutoff of 40 m/s, parent body true anomaly  $f = 30^\circ$  and argument of perihelion  $\omega = 150^\circ$ . This curve was defined by Tsiganis et al. (2007) as that closest to representing the dispersion of the real Veritas family in orbital element space.

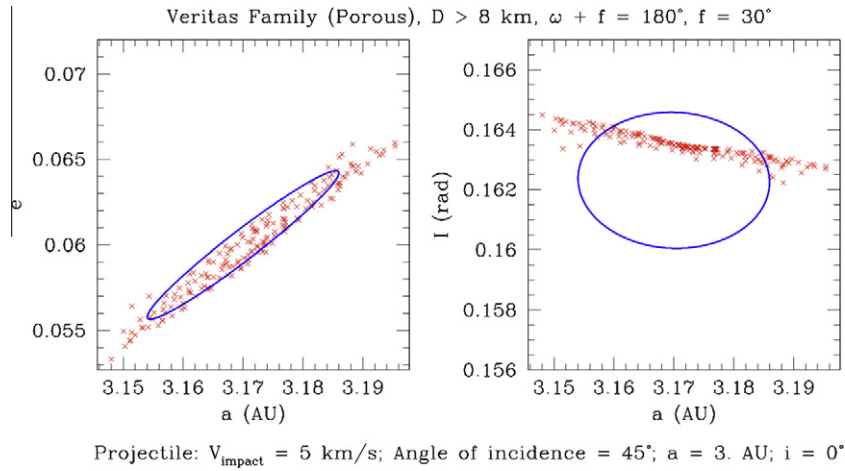


Fig. 5. Same as Fig. 4 for a porous monolithic parent body.

the (5, −2, −2) Jupiter–Saturn–asteroid three-body resonance in such a way that it does not converge with the rest of the family members at −8.3 Myr. But strangely enough, the resonance produces chaotic diffusion that agrees with that age. However, when viewed in the Nata frame, there is a possibility that Veritas is an interloper. Mothéz-Diniz et al. (2005) found that when identified using cutoff values smaller than 28 m/s, the family remains detected, possibly linking artificially to the family small asteroids located at low inclinations in the (5, −2, −2) resonance due to limitations of the HCM method (see footnote 1), but (490) Veritas is no longer one of its members. The main member instead is the second-largest one, (1086) Nata. The cluster around (1086) Nata reduces to only 17 bodies at cutoff 8 m/s. The fact that this cluster can be detected at such small cutoffs has been interpreted as the consequence of the recent collisional breakup—about 8.2 Myr ago—of an asteroid in that region of the belt (Nesvorný et al., 2003).

These arguments motivated us to explore whether we could reproduce a Veritas family, excluding the Asteroid Veritas itself from the family members. Some other small asteroids at low inclinations in the (5, −2, −2) resonance should probably also be excluded, as explained above, but given their small size and the fact that our main concern is with the large-size end of the collisional outcome, they should not affect our conclusions. In this case, the parent body’s size has to be reduced, accounting for the absence of the Asteroid Veritas. Table 2 shows the initial conditions of the simulations, using both a non-porous and a porous parent body whose diameter has been reduced to 112 km. Note that Farley et al. (2006) related a late Miocene dust shower to the breakup at the origin of the Veritas family about 8 Myr ago. They estimated that the disruption of the family parent body, supposed to be greater than 150 km in diameter, could produce a transient increase in the flux of interplanetary dust-derived <sup>3</sup>He. However, since the

amount of dust produced during an asteroid disruption is badly constrained (as it is well below the resolution limit of any simulation), a parent body diameter of 112 km is likely still consistent with this scenario.

#### 4.1. Size distribution of family members

Fig. 6 shows the size distributions resulting from the disruption of monolithic parent bodies. Starting from a non-porous parent body, the resulting fragment size distributions are totally different from that of the real family. Such a discrepancy that results from using the non-porous parent body is not necessarily a surprise, given the dark taxonomic type of the family, which is consistent with a porous parent body. On the other hand, starting from a porous parent body, the match is actually spectacular. Note that the fall-off in the observed members at small sizes can be attributed to the observational completeness limit. Both the largest and second-largest remnants are very well reproduced, as is the slope at smaller sizes. Similar results are found when starting with pre-fragmented parent bodies (Fig. 7), although the quality of the match is lower than when starting from monolithic parent bodies.

This remarkable match makes us conclude that the Veritas family may contain an important interloper, i.e. Veritas itself, which is in fact the asteroid after which it was initially named, and possibly a few other small ones located around it in proper-element space. This is also consistent with some of the analyses performed in the studies mentioned earlier (e.g. Mothéz-Diniz et al., 2005).

#### 4.2. Orbital distribution of family members

As we did in Section 3.2, we computed the orbital distribution of our simulated families. Figs. 8 and 9 show the results starting from a non-porous and a porous monolithic parent body, respectively, impacted head-on. Both match the shape of the ellipses representing the real dispersion. Our statements indicated in Section 3.2 regarding the similarity of the dispersion using pre-fragmented parent bodies hold true. However, in the present case, the dispersion from the non-porous parent body remains narrow compared to the real one, while the one from a porous parent body could also be fitted by larger ellipses to contain all fragments. Note that some real members are also outside those ellipses (see Fig. 1 in Tsiganis et al. (2007)) and that in the latter case, we found that values of the angle β (see Section 3.2) in the range 50–90° do not change the shape and extent of the dispersion much. Using a smaller value concentrates all fragments in the center of the ellipse. So,

**Table 2**  
Parameters used for simulations of the Veritas family formation but excluding Asteroid Veritas itself. The diameter of the revised parent body (PB) is 112 km.

Composition	Structure	$R_p$ (km)	$\theta$ (°)	$Q$ (erg/g)	$M_{ir}/M_{pb}$
Non-porous	M	10	0	$7.10 \times 10^8$	0.42
Non-porous	M	14	45	$1.95 \times 10^9$	0.20
Porous	M	10	0	$7.10 \times 10^8$	0.21
Porous	M	14	45	$1.95 \times 10^9$	0.18
Non-porous	PF	10	0	$7.10 \times 10^8$	0.10
Non-porous	PF	14	45	$1.95 \times 10^9$	0.27
Porous	PF	10	0	$7.10 \times 10^8$	0.23
Porous	PF	14	45	$1.95 \times 10^9$	0.22

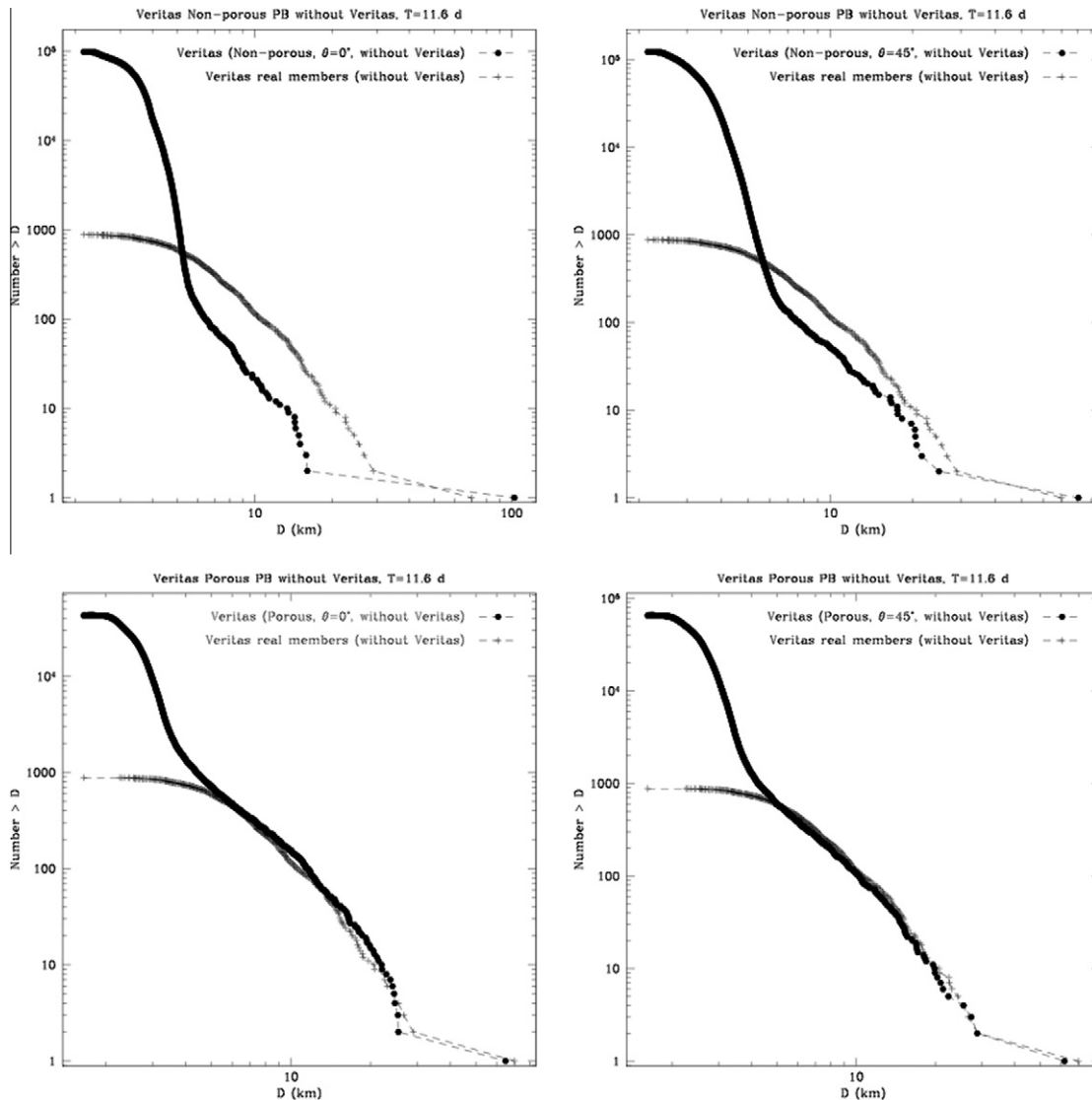


**Fig. 6.** Cumulative size distributions of fragments from the simulations of the disruption of a Veritas monolithic parent body, either non-porous or porous. Impact angles are  $0^\circ$  or  $45^\circ$  and the impact speed is 5 km/s. The distribution of the real family is also shown for comparison. In this case, the family consists of all members except Veritas itself, which reduces the size of the parent body to 112 km. The simulated time is about 11.6 days after the impact.

apparently in this case, this angle has more influence for unclear reasons. But this result shows that the orbital extent of the family does not have to be produced by post-diffusion processes, because for some values of  $\beta$  we find a good match using a porous parent body.

Fig. 10 shows the result starting from a monolithic porous body impacted at  $45^\circ$ . With this impact angle, the disruption of a non-porous parent body leads to an orbital distribution mostly outside of the ellipses shown on those figures. Fig. 10 shows the same kind of dispersion as in the case where we considered Veritas as a family member (and a larger parent body) using the same impact angle (see Section 3.2, Fig. 5).

Therefore, considering both the size distribution and orbital dispersion, the best (and almost perfect) match that we find is from the disruption of a porous parent body of the family without Veritas, impacted head-on.

## 5. Discussion

Given the very good match of our simulations of a porous body disruption when we exclude the Asteroid Veritas from its family,

we conclude that Veritas may not belong to the family identified under its name. Another, and probably better, way to say it is that the Asteroids (1086) Nata and (490) Veritas do not seem to belong to the same size distributions. That way, we leave open the possibility that an asteroid family was produced, with Nata as the largest member, which would correspond to our scenario presented in Section 4, which does not rule out the possibility that another disruption produced Veritas as the largest fragment followed by only much smaller fragments located around it in proper-element space.

On the basis of dynamical considerations, Nesvorný et al. (2003) already indicated the existence of a tight group around the second-largest member of the family, (1086) Nata. They found it plausible that a breakup of a smaller family member within Veritas occurred about 8.3 Myr ago and formed (1086) Nata as well as the other family members that contribute to this tight group. On the other hand, it may be that the age corresponds to the whole family, as proposed by Tsiganis et al. (2007), and that a way to reconcile both interpretations is simply to exclude Veritas, as our simulations suggest, or to invoke the possibility that we have two distinct tight groups of the same age. In fact, Tsiganis et al. (2007) stated that the equivelocity curves were drawn as to contain only the dynamically



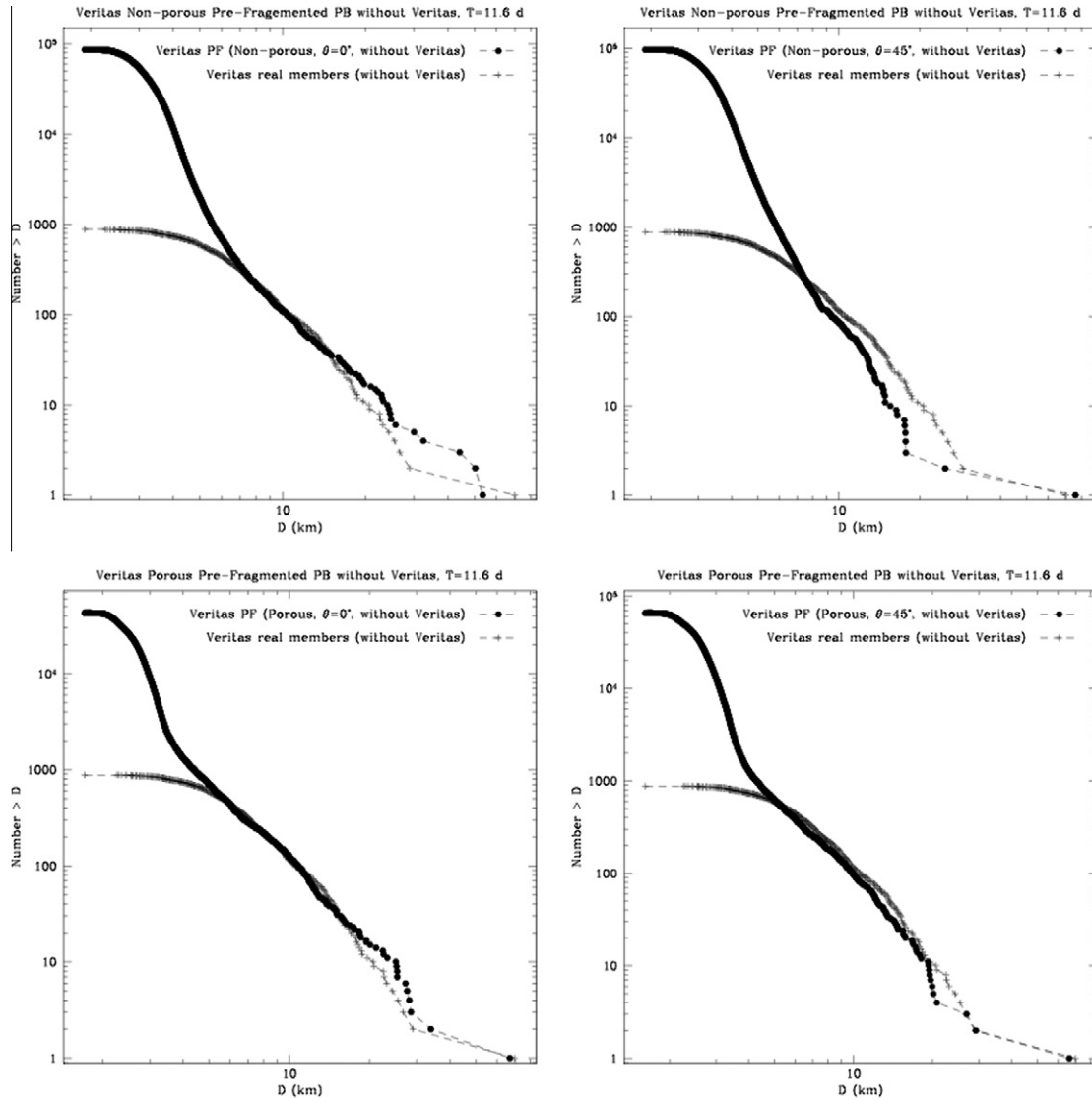


Fig. 7. Same as Fig. 6, but for the disruption of pre-fragmented (PF) parent bodies.

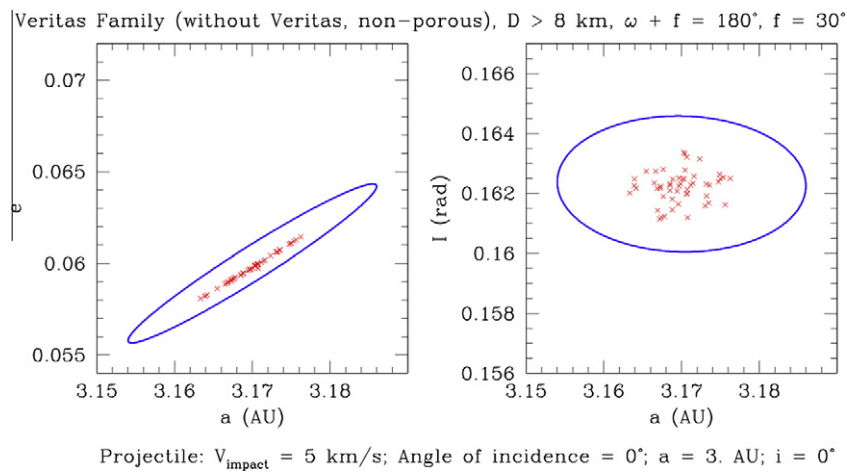
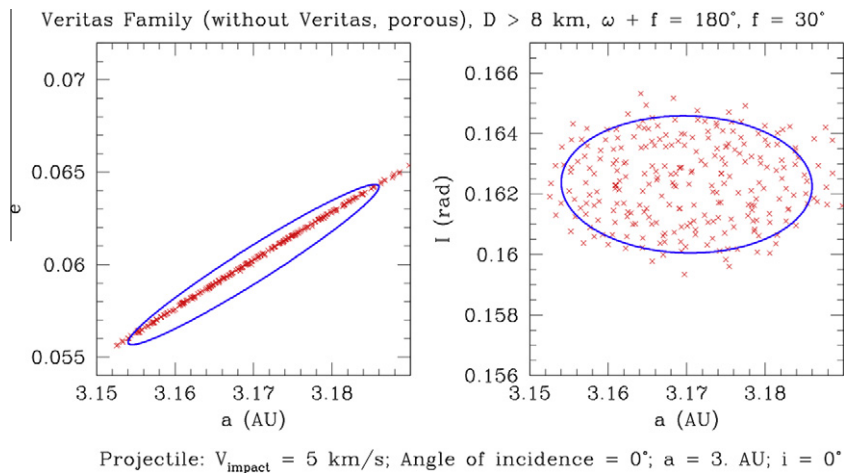


Fig. 8. Same as Fig. 4 but starting from a non-porous monolithic parent body of the Veritas family that excludes the Asteroid Veritas from the membership;  $\beta = 90^\circ$  and the impact angle is  $0^\circ$ .

regular component of the family, and thus, many resonant objects were out of the ellipses because of their large dispersion in the

eccentricity-inclination plane. These deviations were then used to estimate the age, assuming that the initial spread was given



**Fig. 9.** Same as Fig. 8, but starting from a porous monolithic parent body and excluding Veritas itself.

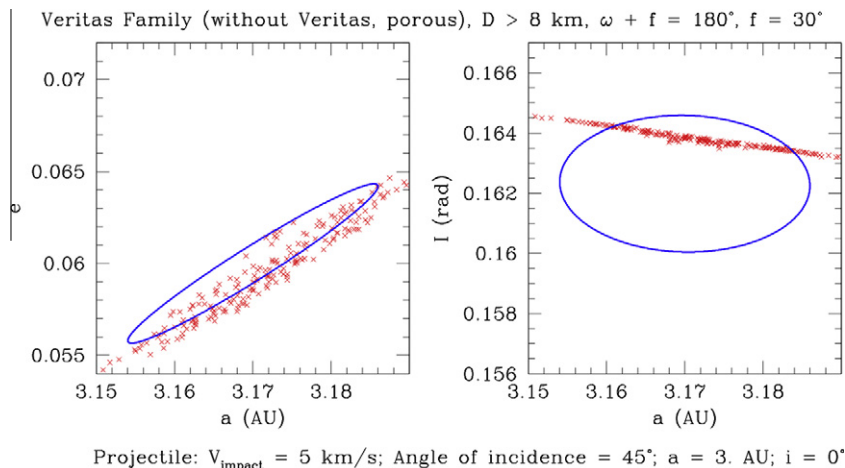


**Fig. 10.** Same as Fig. 9 but for a projectile impact angle of  $45^\circ$ . Many fragments lie outside of these figures and therefore the orbital dispersion is much greater than that corresponding to the ellipses.

by the equivelocity curves and the resonant members evolved to what we see due to chaotic diffusion. This initial spread is well reproduced by several of our simulations, as shown in previous sections. Then, the existence of a low-inclination group was already suspected near the semi-major axis of Veritas, but could not be firmly established because the asteroid catalog contained fewer bodies than presently. Thus, the possibility of two distinct groups exists, one of them including Veritas and much smaller bodies, the other one including Nata as the largest member and other bodies. Our simulations reproducing well the family with Nata as the largest fragment in terms of both size and velocity distributions are consistent with the existence of the second group and therefore give additional arguments in favor of this possibility.

Regarding compositional aspects, based on spectroscopic observations, it was found by Di Martino et al. (1997) that some large family members whose spectra have been characterized have a flat spectrum typical of C-type asteroids, but that the spectrum also contains a shallow and wide absorption band center at 700 nm, which is not found in the Veritas spectrum. The authors noted that it remains difficult to explain why the largest remnant of the family (490 Veritas) does not present the same feature. A compositional diversity within the parent body cannot be ruled out, but this discrepancy in spectral features is at least not in contradiction with our suggestion that Veritas does not belong to its family as

originally defined. Note that, contrary to di Martino et al. (1997), Mothéz-Diniz et al. (2005) found that the Veritas family is actually a rather homogeneous C-type family and classified the previous X/D-type spectrum of Veritas by di Martino et al. (1997) as a Ch-type. As suggested by Mothéz-Diniz et al. (2005), we encourage observers to perform additional spectral observations of this family, including Veritas, to have a more detailed understanding of spectral differences within this cluster of bodies.

## 6. Conclusion

We have performed numerical simulations of the formation of the Veritas family, using both a non-porous and a porous parent body and a projectile impacting at 3 or 5 km/s with an impact angle of  $0^\circ$  or  $45^\circ$ . Not one of these simulations was able to produce satisfactorily the estimated size distribution of real family members. The chosen impact conditions, in particular the impact speeds, are considered to be the most probable ones in the main belt (Bottke et al., 1994). Therefore, even if we cannot rule out that some impact conditions may allow a good match, they may not correspond to likely ones, and the parameter space is too large to look for such unlikely conditions, if they exist. Based on previous studies devoted to either the dynamics or the spectral properties

of the Veritas family (e.g., Nesvorný et al., 2003; Mothéz-Diniz et al., 2005), which already treated (490) Veritas as a special object that may be disconnected from the family, we simulated the disruption of a family consisting of the full family without that asteroid. In that case, the parent body is smaller (112 km in diameter), and we found a remarkable match of the simulation outcome from a porous parent body with the real family. Both the size distribution and the velocity dispersion of the real reduced family are remarkably well reproduced. The best match is obtained with a head-on impact. On the other hand, the disruption of a non-porous parent body does not reproduce the observed properties very well. This is consistent with the spectral C-type of family members, which suggests that the parent body was porous and shows the importance of modeling the effect of this porosity in the fragmentation process, even if the largest members are produced by gravitational reaccumulation during the subsequent gravitational phase.

As a result of our investigations, we conclude that it is very likely that the Asteroid (490) Veritas and probably several other small members do not belong to the family as originally defined, and that the definition of this family should be revised. Also, we note that there are some discrepancies between spectral observations made by di Martino et al. (1997) and Mothéz-Diniz et al. (2005) for the same objects. As recognized by the later authors, these differences need additional observations to be understood, and our study motivates this even more.

Numerical simulations of family formation and observations can then serve the same cause, i.e. defining asteroid families more robustly. Such families can help us better understand the disruption process at large scales. Their numbers and properties give us some hints on the collisional history of the main belt and the delivery of meteorites to the Earth. Further investigations will be performed to better constrain the definitions and properties of asteroid families of different types, using the appropriate model of fragmentation.

## Acknowledgments

We are grateful to David Nesvorný for having provided us the current observed family data and useful comments regarding their interpretation. We also thank Kleomenis Tsiganis and David P. O'Brien for their constructive reviews. P.M. acknowledges financial support from the French Programme National de Planétologie and from the Japan Society for the Promotion of Science (JSPS) Invitation Fellowship for Research 2009. M.J. and P.M. acknowledge support from the French-Japanese Cooperation Program CNRS-JSPS 2008-2009. D.C.R. acknowledges support from the National Aeronautics and Space Administration under Grant No. NNX08AM39G issued through the Office of Space Science.

## References

Benz, W., 1990. Smooth particle hydrodynamics—A review. In: Buchler, J.R. (Ed.), *The Numerical Modeling of Non-Linear Stellar Pulsations: Problems and Prospects*, p. 269.

Benz, W., Asphaug, E., 1994. Impact simulations with fracture. I. Method and tests. *Icarus* 107, 98–116.

Benz, W., Asphaug, E., 1995. Simulations of brittle solids using smooth particle hydrodynamics. *Comput. Phys. Commun.* 87, 253–265.

Bottke, W.F., Nolan, M.C., Greenberg, R., Kolvoord, R.A., 1994. Velocity distributions among colliding asteroids. *Icarus* 107, 255–268.

Bottke, W.F., Vokrouhlický, D., Nesvorný, D., 2007. An asteroid breakup 160 Myr ago as the probable source of the K/T impactor. *Nature* 449, 48–53.

Britt, D.T., Consolmagno, G.J., 2000. The porosity of dark meteorites and the structure of low-albedo asteroids. *Icarus* 146, 213–219.

Carroll, M.M., Holt, A.C., 1972. Suggested modification of the P- $\alpha$  model for porous materials. *J. Appl. Phys.* 43, 759–761.

di Martino, M., Migliorini, F., Zappalà, V., Manara, A., Barbieri, C., 1997. Veritas asteroid family: Remarkable spectral differences inside a primitive parent body. *Icarus* 127, 112–120.

Durda, D.D., Bottke, W.F., Nesvorný, D., Enke, B.L., Merline, W.J., Asphaug, E., Richardson, D.C., 2007. Size frequency distributions of fragments from SPH/N-body simulations of asteroid impacts: Comparison with observed asteroid families. *Icarus* 186, 498–516.

Farley, K.A., Vokrouhlický, D., Bottke, W.F., Nesvorný, D., 2006. A late Miocene dust shower from the break-up of an asteroid in the main belt. *Nature* 439, 295–297.

Grady, D.E., Kipp, M.E., 1980. Continuum modeling of explosive fracture in oil shale. *Int. J. Rock Mech. Min. Sci. Geomech. Abstr.* 17, 147–157.

Herrmann, W., 1969. Constitutive equation for the dynamic compaction of ductile porous materials. *J. Appl. Phys.* 40, 2490–2499.

Housen, K.R., Holsapple, K.A., Voss, M.E., 1999. Compaction as the origin of the unusual craters on the Asteroid Mathilde. *Nature* 402, 155–157.

Jutzi, M., Benz, W., Michel, P., 2008. Numerical simulations of impacts involving porous bodies. I. Implementing sub-resolution porosity in a 3D SPH hydrocode. *Icarus* 198, 242–255.

Jutzi, M., Michel, P., Hiraoka, K., Nakamura, A.M., Benz, W., 2009. Numerical simulations of impacts involving porous bodies. II. Confrontation with laboratory experiments. *Icarus* 201, 802–813.

Jutzi, M., Michel, P., Benz, W., Richardson, D.C., 2010. The formation of the Baptistina family by catastrophic disruption: Porous versus non-porous parent body. *Meteorit. Planet. Sci.* 44, 1877–1887.

Knežević, Z., Pavlovic, R., 2002. Young age for the Veritas asteroid family confirmed? *Earth Moon Planets* 88, 155–166.

Libesky, L.D., Petschek, A.G., 1991. Smooth particle hydrodynamics with strength of materials. In: Trease, H.E., Fritts, M.F., Crowley, W.P. (Eds.), *Proc. Next Free-Lagrange Method, Lecture Notes in Physics*, vol. 395. Springer-Verlag, Berlin, pp. 248–257.

Michel, P., 2003. Modelling collisions between asteroids: From laboratory experiments to numerical simulations. *Lect. Notes Phys.* 682, 117–143.

Michel, P., Benz, W., Tanga, P., Richardson, D.C., 2001. Collisions and gravitational reaccumulation: Forming asteroid families and satellites. *Science* 294, 1696–1700.

Michel, P., Benz, W., Tanga, P., Richardson, D.C., 2002. Formation of asteroid families by catastrophic disruption: Simulations with fragmentation and gravitational reaccumulation. *Icarus* 160, 10–23.

Michel, P., Benz, W., Richardson, D.C., 2003. Disruption of fragmented parent bodies as the origin of asteroid families. *Nature* 421, 608–611.

Michel, P., Benz, W., Richardson, D.C., 2004a. Disruption of pre-shattered parent bodies. *Icarus* 168, 420–432.

Michel, P., Benz, W., Richardson, D.C., 2004b. Catastrophic disruption of asteroids and family formation: A review of numerical simulations including both fragmentation and gravitational reaccumulations. *Planet. Space Sci.* 52, 1109–1117.

Milani, A., Farinella, P., 1994. The age of the Veritas asteroid family deduced by chaotic chronology. *Nature* 370, 40–42.

Mothéz-Diniz, T., Roig, F., Carvano, J.M., 2005. Reanalysis of asteroid families structure through visible spectroscopy. *Icarus* 174, 54–80.

Nakamura, A.M., Fujiwara, A., 1991. Velocity distribution of fragments formed in a simulated collisional disruption. *Icarus* 92, 132–146.

Nesvorný, D., Morbidelli, A., 1998. Three-body mean motion resonances and the chaotic structure of the asteroid belt. *Astron. J.* 116, 3029–3037.

Nesvorný, D., Morbidelli, A., 1999. An analytic model of three-body mean motion resonances. *Celest. Mech. Dynam. Astron.* 71, 243–271.

Nesvorný, D., Bottke, W.F., Levison, H.F., Dones, L., 2003. Recent origin of the Solar System dust bands. *Astrophys. J.* 591, 486–497.

Nohakovic, B., Tsiganis, K., Knežević, Z., 2010. Chaotic transport and chronology of complex asteroid families. *Mon. Not. R. Astron. Soc.* 402, 1263–1272.

Öpik, E.J., 1951. Collision probabilities with the planets and the distribution of interplanetary matter. *Proc. R. Irish. Acad.* 54, 165–199.

Richardson, D.C., 1994. Tree code simulations of planetary rings. *Mon. Not. R. Astron. Soc.* 269, 493–511.

Richardson, D.C., Quinn, T., Stadel, J., Lake, G., 2000. Direct large-scale N-body simulations of planetesimal dynamics. *Icarus* 143, 45–59.

Richardson, D.C., Michel, P., Walsh, K.J., Flynn, K.W., 2009. Numerical simulations of asteroids modeled as gravitational aggregates with cohesion. *Planet. Space Sci.* 57, 183–192.

Stadel, J., 2001. *Cosmological N-body Simulations and Their Analysis*. Ph.D. Thesis, University of Washington, Seattle, 126 pp.

Tillotson, J.H., 1962. *Metallic Equations of State for Hypervelocity Impact*. General Atomic Report GA-3216, July 1962.

Tsiganis, K., Knežević, Z., Varvoglis, H., 2007. Reconstructing the orbital history of the Veritas family. *Icarus* 186, 484–497.

Yeomans, D.K. et al., 1997. Estimating the mass of Asteroid 253 Mathilde from tracking data during the NEAR flyby. *Science* 278, 2106–2109.

Zappalà, V., Bendjoya, Ph., Cellino, A., Farinella, A., Froeschlé, C., 1995. Asteroid families: Search of a 12, 487 asteroid sample using two different clustering techniques. *Icarus* 116, 291–314.